Search for GRB neutrinos via a (stacked) time profile analysis

Martijn Duvoort* **and Nick van Eijndhoven*** **for the IceCube collaboration†**
*University of Utrecht, The Netherlands
†see special section of these proceedings

***Abstract*. An innovative method to detect high-energy neutrinos from Gamma Ray Bursts (GRBs) is presented. The procedure provides a good sensitivity for both prompt, precursor and afterglow neutrinos within a 2 hour time window around the GRB trigger time. The basic idea of the method consists of stacking of the observed neutrino arrival times with respect to the corresponding GRB triggers. A possible GRB neutrino signal would manifest itself as a clustering of signal candidate events in the observed time profile. The stacking procedure allows to identify a signal even in the case of very low rates.**

We outline the expected performance of analysing four years of AMANDA data (2005–2008) for a sample of 130 GRBs. Because of the extreme optical brightness of GRB080319B, it might be that this particular burst yielded multiple detectable neutrinos in our detector. As such, the method has also been applied to the data of this single burst time profile. The results of this analysis are presented in a separate section.

***Keywords*: GRB Neutrinos AMANDA/IceCube**

I. Introduction

Gamma Ray Bursts are among the most promising sources for high-energy neutrino detection: the accurate localization and timing information presently available, enable very effective background reduction for high-energy neutrino detectors. Yet, no previous search for GRB neutrinos has led to a discovery [1], [2]. As most models of a GRB jet predict neutrino formation simultaneous with the prompt γ emission, previous analyses aim to discover neutrinos that arrive simultaneously with the prompt photons. However, it might be that the main GRB neutrino signal is not simultaneous with the prompt gammas, either in production or arrival at the Earth.

A variety of the models predict the formation of high-energy neutrinos at different stages in the evolution of a GRB. Afterglow models predict a significant neutrino flux a few seconds after the prompt emission [3], [4]. The existence of multiple colliding shells in a GRB jet [5] may also lead to a time difference between high-energy gamma emission and neutrinos. Even if the neutrinos and photons are produced at the same stage of the evolution of the GRB jet, a time difference at the observer may be present: as the jet evolves, it will become transparent for photons at a later stage than for neutrinos. Therefore, neutrinos might be able to escape the source region well before the high-energy photons. This will depend heavily on the actual stage in the evolution of the jet.

For our analysis we use the data of the AMANDA-II detector at the South Pole [6] to look for a neutrino signal. Our analysis method is aimed to be less model dependent than previous GRB analyses. It is insensitive to a possible time difference between the arrival of the prompt photons and the high-energy neutrino signal. We limit the dependence on the expected neutrino spectrum by not using any energy dependent selection criteria. We only use directional selection parameters based on the reconstructed muon track, resulting from an incident muon neutrino [6]. As the detectable number of signal neutrinos in our detector per GRB is very low [7] ($\ll 1$), our method is designed to allow for gaining sensitivity to a GRB neutrino signal by stacking neutrino data of multiple GRBs around their trigger time. Those stacked time profiles can be analysed using the same techniques as the time profile of a single GRB. We first outline the analysis method itself, then we give the results of applying this method to GRB080319B, the most luminous GRB observed to date.

II. The analysis method

We look for signal events correlated with the GRB direction and time. As the background of our detector, which consists of cosmic ray events, is not correlated, we start by filtering the data for a GRB coincidence, both spatially and temporally. The exact selection parameters we use are optimized as outlined in section III.

The GRB data that passes the cuts has a certain time-distribution with respect to the GRB trigger time. The background events that pass the cuts will be uniformly distributed in time with respect to the GRB trigger. A possible GRB signal will be clustered in time. Note that this argument also holds for the case of stacking multiple GRB time windows, which is the main purpose of this analysis method. Here we assume that the intrinsic time difference between photons and neutrinos is a characteristic feature for all GRBs in our sample. Obviously we aim to have all GRB signal neutrinos ending up in the same time-bin. Therefore, the usage of a too small time bin will reduce the sensitivity as signal entries will end up in different bins. Using a too large time bin also reduces the sensitivity as background entries will start to dominate the bins. We estimate the timespread of the neutrino signal to be of the same order of the observed photonic GRB duration: the T_{90} time, defined as the time in which $5\% - 95\%$ of the GRB fluence was detected. This is a safe estimate as the intrinsic

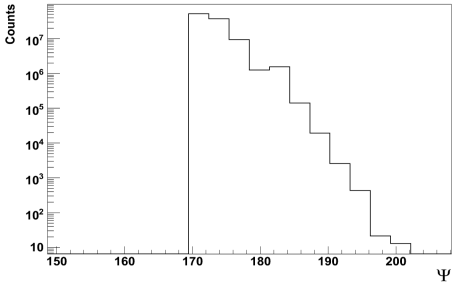

Fig. 1. The Ψ distribution for randomizing 13 entries in 120 bins. (10^8 randomizations)

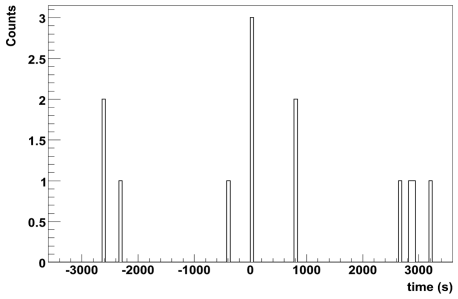

Fig. 2. The time distribution of 3 signal events (at $t = 0$) and 10 randomly distributed events in a 2 hour window using 60 s bin size.

timespread of the neutrino signal will not be larger than that of the photons: as the source region will always be more opaque for photons than for neutrinos, the photon signal will spread more in time than the neutrino signal. We have chosen a conservative bin size of 60 s, resulting in 120 time bins in our 2 hour window.

The probability of observing a certain time distribution given a uniform background distribution, of in total n entries divided over m time bins, is given by the multinomial distribution [8]:

$$p(n_1, n_2, ...n_m|nm) = \frac{n!}{n_1! \cdots n_m!} p_1^{n_1} \cdots p_m^{n_m} \equiv p. \quad (1)$$

Here p_i is the probability of an entry ending up in bin i. In case of a uniform background this is simply m^{-1}. The n_i represents the number of entries in bin i. We derive the bayesian $\Psi \equiv -10 \log p$ [9]:

$$\Psi = -10 \left[\log n! + \sum_{k=1}^{m} (n_k \log p_k - \log n_k!) \right]. \quad (2)$$

If the observation is due to the expected background, a low Ψ value will be obtained. Deviations from the expected background will result in increased Ψ values.

We intend to compare the Ψ value of the observed data, including a possible signal, with the distribution of uniform background Ψ values. We obtain such background sets by (uniformly) randomizing the entries in the two hour time window, keeping the total number of entries constant to what we find in the data. In case of a large signal contribution, this may result in underestimating the significance of the signal. However, for such a high signal contribution we will be able to claim discovery anyway. To claim a discovery we require at least a 5σ level, which means that only a fraction of 5.73×10^{-7} (the corresponding P-value) of all the Ψs of the various background sets is allowed to exceed some threshold Ψ_0. In case the Ψ value of our observed data is larger than Ψ_0, we have a discovery.

In order to reach the necessary accuracy, we perform 10^8 randomizations of all the data events that pass the criteria and calculate the Ψ value of each randomization to obtain a background Ψ distribution. In figure 1 we give one example of our parameter space. Here $n = 13$ entries exist in our simulated observation time window of 120 bins.

As an example, one might observe a time distribution, consisting of 3 signal events in a single bin and 10 randomly distributed background entries, which is shown in figure 2. The Ψ value associated with this distribution equals 186.15. When comparing with the background Ψ distribution of figure 1 it becomes clear that this corresponds to a P-value of 1.13×10^{-3} above the observed $\Psi_0 = 186.15$. For a 5σ discovery we need this fraction to be less than 5.73×10^{-7}. Therefore, observing a time profile like figure 2 will not result in a significant discovery.

III. Optimization of the selection parameters

The significance of our observation is determined by the method outlined in section II. Before we do this we need to optimize the directional parameter values which we use for selecting the final event sample by means of a blind analysis. In order to stay comparable to previous analyses, we will use the standard Model Discovery Factor (MDF) [10], [11] to determine the optimum of our parameter space. At those optimal settings the standard Model Rejection Factor (MRF) [12] is calculated.

The average expected number of background counts per time bin μ_b is calculated by simply dividing the total number of observed entries in the time window by the number of time bins. This is justified by the assumption that the expected signal is much smaller than the background $\mu_\mathrm{b} \gg \mu_\mathrm{s}$. We optimize the selection parameters for a 5σ discovery. The significance we use in the calculation of the MDF is corrected for a trial factor due to the number of bins.

By systematically going through the grid of our parameter space, we reach the parameter values corresponding to a minimum MDF, i.e. we optimize our analysis for discovery. In case of no discovery, the MRF at these settings will provide a flux upper limit. Since we optimize our parameters on the randomized data itself, our background set consists of randomized background plus signal entries. For parameter settings where less than four entries pass, the Ψ statistics cannot result in a discovery: all possible P-value exceed 5.73×10^{-7}. Therefore, we require that at our optimal thresholds, at least four events pass our filter. This is achieved by slightly relaxing the selection criteria.

IV. THE GRB080319B AMANDA ANALYSIS

Even though the expected number of signal neutrinos for an average GRB is extremely low, the atypical GRB080319B might yield an unusually strong neutrino signal justifying an individual neutrino analysis. The analysis of IceCube data [13] was confined to 10 minutes around the GRB trigger time. No neutrino signal was found. We analyse a larger data block from one hour before till one hour after the trigger time, and use the same spectrum as in [13] for our optimization and limit:

$$\frac{dN_\nu}{dE_\nu} = \begin{cases} 6.620 \times 10^{-16} \times E_\nu^{0.59} & \text{if } E_\nu \leq E_1; \\ 0.768 \times E_\nu^{-2.145} & \text{if } E_1 \leq E_\nu \leq E_2; \\ 6.690 \times E_\nu^{-4.145} & \text{if } E_\nu \geq E_2, \end{cases} \tag{3}$$

with the fluence, dN_ν/dE_ν, in (GeV cm^2)$^{-1}$ and the break energies: $E_1 = 322.064$ TeV; $E_2 = 2952.35$ TeV.

For our time profile we use a bin size of 60 s, roughly the T_{90} of this burst. While we expect this to be wide enough for the GRB neutrino signal to fit in one bin, a possible neutrino signal can be spread over two adjacent bins. This obviously lowers the significance of the observation. Therefore, in case we do not find a 5σ result with our initial analysis, we compensate for this binning effect by performing our analysis a second time, where we shift our bins by half a binwidth.

Using a simulated neutrino fluence following the spectrum (3), we obtain the optimum of our parameter space following the method of section III. We find at the optimal parameter settings a 5σ MDF of 123.65 and have six events passing the filter. Based on the GRB spectrum we expect 0.064 signal entries to pass the filter. We find (at 90% confidence level) an MRF of 38.8 for the GRB spectrum. Likewise, using a generic E^{-2} spectrum, we obtain at these settings a limit of $E^2 dN_\nu/dE_\nu = 1.11 \times 10^{-2}$ (GeV cm^2 s)$^{-1}$ at 90% confidence level. Note that these limits are conservative as the Ψ statistics we use to claim discovery is more sensitive than the Poisson statistics on which the MRF is based.

The previous analysis of IceCube data [13] quotes a sensitivity at a fluence of 22.7 times the expected spectrum at 90% C.L. for prompt emission. We find a 90% C.L. limit at 38.8 times the expected spectrum for a neutrino signal arriving in the central bin. This difference

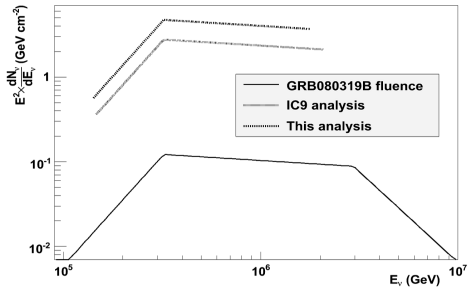

Fig. 3. The 90% C.L. upper limits on the fluence of GRB080319B with respect to the calculated neutrino fluence (3) for both this analysis and the IceCube analysis in its 9 string configuration.

can be seen in figure 3, where the limits of both analyses are given.

The neutrino effective areas for the AMANDA detector for this analysis are given in figure 4. It is given at

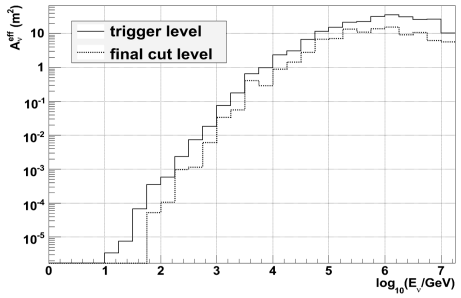

Fig. 4. The neutrino effective area for the position of GRB080319B, both at trigger level and at final cut level.

both trigger level and at the level where all our selections have been applied. The ratio between the 2 histograms is the signal passing rate, which, for the GRB spectrum (3), equals 49.4%.

The time profile we find after unblinding is consistent with the background-only hypothesis. Repeating the analysis with shifted time bins does not change this.

V. THE STACKING ANALYSIS

In this section we present the expected results of analysing the stacked AMANDA data of 130 GRBs between 2005 and 2008. These well-localized bursts are all in the Northern hemisphere to reduce the background due to atmospheric events. The time profile of each GRB is sampled to form a stacked time profile.

Due to the different redshifts of the GRBs in the sample, the effect of cosmological time dilation on the intrinsic time difference between photons and neutrinos will result in a timespread on the arrival of the neutrino signal. This spread will increase for larger time differences. We compensate for this by enlarging the bin sizes for bins further away from the trigger. Each bin will be enlarged by a factor of $\langle z \rangle + 1$, where $\langle z \rangle$ is the average redshift of the GRBs in our sample. We choose to have our central bin range from $-\langle T_{90} \rangle \approx -30$ s to $\langle T_{90} \rangle \approx 30$ s, allowing for a scatter in the neutrino arrival time of the average length of the photon signal. The second bin is a factor of $\langle z \rangle + 1 \approx 3$ larger than the maximum scatter we allow in the center bin and ranges $[30, 120]$ s (and $[-120, -30]$ s). The next bin is again a factor of 3 larger.

The fact that the bins in our time window have unequal sizes does not influence our method. It is simply taken into account by using, for each bin, the correct p_i, the probability for an entry to fall in that bin, see equation (2). Let us consider the same time profile as above (figure 2) with these new bin settings. This leads to the time profile as given in figure 5. Because our time window now has variable binning, the configuration itself changed significantly with respect to the regular

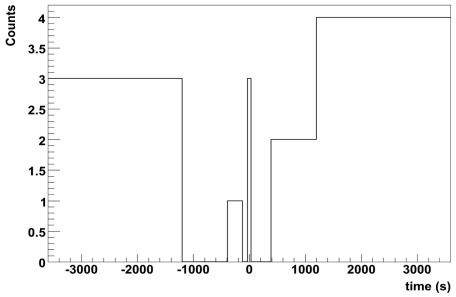

Fig. 5. The time distribution of 3 signal events and 10 randomly distributed events in a 2 hour window. Here we use nine variable time bins as explained in the text.

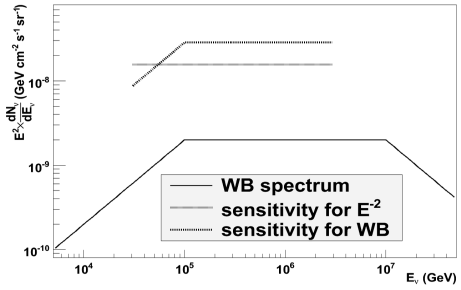

Fig. 6. The sensitivity of this analysis for both a generic E^{-2} and a Waxman-Bahcall (WB) source spectrum (90% C.L.).

case of figure 2. Hence the new Ψ value of our observation (63.44) differs from the previously found value. The background Ψ distribution of figure 1 will change accordingly. Following our example, one can study the

$n_{\rm signal}$	P-value regular 60 s bins	P-value variable bins
1	6.32×10^{-2}	2.36×10^{-1}
2	9.67×10^{-3}	3.77×10^{-2}
3	1.13×10^{-3}	3.14×10^{-3}
4	2.71×10^{-5}	1.80×10^{-4}
5	1.1×10^{-6}	7.8×10^{-6}
6	1×10^{-8}	2.2×10^{-7}

TABLE I
COMPARISON BETWEEN THE SIGNIFICANCE FOR THE CASE OF THE TIME PROFILE OF FIGURE 2 AND THE SAME SITUATION USING THE VARIABLE BINS AS IN FIGURE 5. HERE WE VARY THE AMOUNT OF SIGNAL ENTRIES IN THE CENTER BIN $n_{\rm signal}$; THE 10 BACKGROUND ENTRIES ARE LEFT UNTOUCHED.

effect of the variable binning on the significance of our time profile for different signal strengths. From table I one can see that introducing variable bin sizes slightly lowers the significance of our observations (their P-value) for a signal falling in the center bin.

For the optimization of the selection parameters we use both a Waxman-Bahcall and a generic E^{-2} spectrum. Again, we optimize for discovery using the standard MDF. As a result from the various binsizes, the limit of this analysis depends on the bin size, and therefore depends on the time difference with the GRB trigger. The sensitivity of this analysis for each bin in our

Time range w.r.t. GRB trigger	WB spectrum at 1 PeV (GeV cm^2 s sr)$^{-1}$	$E^2 dN_\nu/dE_\nu$ (GeV cm^2 s sr)$^{-1}$
$[-30, 30]$ s	2.9×10^{-8}	1.55×10^{-8}
$\pm$ [30, 120] s	3.0×10^{-8}	1.58×10^{-8}
$\pm$ [120, 390] s	3.3×10^{-8}	1.76×10^{-8}
$\pm$ [390, 1200] s	4.2×10^{-8}	2.24×10^{-8}
$\pm$ [1200, 3600] s	5.8×10^{-8}	3.09×10^{-8}

TABLE II
THE 90% C.L. SENSITIVITY OF THE STACKING ANALYSIS FOR EACH TIME BIN, FOR BOTH THE WAXMAN-BAHCALL (WB) AND A GENERIC E^{-2} SPECTRUM.

time window are given in table II. For the central bin we have shown the limits in figure 6. Note that these limits only apply to a neutrino signal arriving simultaneously with the prompt photon emission.

VI. DISCUSSION

Currently, the most restrictive muon neutrino upper limit has been determined by AMANDA at $E^2 dN_\nu/dE_\nu \leq 1.7 \times 10^{-8}$ GeV cm^{-2} s^{-1} sr^{-1} based on a sample of over 400 GRBs and for the Waxman-Bahcall spectrum at 1 PeV [2]. For our analysis no energy dependent selection parameters are used and the optimum of the selection parameters is independent of the source spectrum we use. As such, our analysis is less model dependent and it allows for a possible time difference between photons and neutrinos. Furthermore, the stacking procedure provides sensitivity even in the case of very low individual GRB rates. As such, the present analysis has the potential of detecting precursor and afterglow neutrinos in addition to prompt ones.

The method may also be used to analyse the data of individual GRBs. By construction our method is slightly less sensitive compared to a model dependent analysis of a single time bin. The effective area of the complete IceCube detector will be at least $\sim$150 times larger than AMANDA's [14]. Applying our analysis on one year data of the full IceCube, would result in a sensitivity well below the predicted Waxman-Bahcall spectrum.

REFERENCES

[1] Achterberg, A., et al. 2008, Astrophys. J. 674, 357
[2] Achterberg, A., et al. 2007, Astrophys. J. 664, 397
[3] Waxman, E., & Bahcall, J. N. 2000, Astrophys. J., 541, 707
[4] Dai, Z. G., & Lu, T. 2001, Astrophys. J. 551, 249
[5] Dar, A., & De Rujula, A. 2001, arXiv:astro-ph/0105094
[6] Ahrens, J., et al. 2004, Nucl. Instr. Meth. A 524, 169
[7] Halzen, F., & Hooper, D. W. 1999, Astrophys. J. 527, L93
[8] Gregory, P. C. 2005, Bayesian Logical Data Analysis for the Physical Sciences, Cambridge University Press, UK, 2005
[9] van Eijndhoven, N. 2008, Astropart. Phys. 28, 540
[10] Punzi, G. 2003, Statistical Problems in Particle Physics, Astrophysics and Cosmology, 79
[11] Hill, G. C., Hodges, J., Hughey, B., Karle, A., & Stamatikos, M. 2006, Statistical Problems in Particle Physics, Astrophysics and Cosmology, 108
[12] Hill, G. C., & Rawlins, K. 2003, Astropart. Phys. 19, 393
[13] IceCube Collaboration: R. Abbasi 2009, arXiv:0902.0131
[14] Ahrens, J., et al. 2004, Astropart. Phys. 20, 507